

RSC Advances



This is an *Accepted Manuscript*, which has been through the Royal Society of Chemistry peer review process and has been accepted for publication.

Accepted Manuscripts are published online shortly after acceptance, before technical editing, formatting and proof reading. Using this free service, authors can make their results available to the community, in citable form, before we publish the edited article. This *Accepted Manuscript* will be replaced by the edited, formatted and paginated article as soon as this is available.

You can find more information about *Accepted Manuscripts* in the [Information for Authors](#).

Please note that technical editing may introduce minor changes to the text and/or graphics, which may alter content. The journal's standard [Terms & Conditions](#) and the [Ethical guidelines](#) still apply. In no event shall the Royal Society of Chemistry be held responsible for any errors or omissions in this *Accepted Manuscript* or any consequences arising from the use of any information it contains.

1 **Production, characterization, engine performance and emission characteristics of**
2 ***Croton megalocarpus* and *Ceiba pentandra* complementary blends in a single-cylinder**
3 **diesel engine**

4 A. M. Ruhul^{a,*}, M. A. Kalam^a, H. H. Masjuki^{a,†}, Abdullah Alabdulkarem^b, A. E. Atabani^c, I.
5 M. Rizwanul Fattah^d, M. J. Abedin^a

6 ^aCentre for Energy Sciences, Faculty of Engineering, University of Malaya, 50603 Kuala Lumpur, Malaysia.

7 ^bMechanical Engineering Department, Collage of Engineering, King Saud University, 11421 Riyadh, Saudi
8 Arabia.

9 ^cDepartment of Mechanical Engineering, Faculty of Engineering, Erciyes University, 38039 Kayseri, Turkey.

10 ^dSchool of Mechanical and Manufacturing Engineering, University of New South Wales, Kensington, 2033
11 NSW, Australia.

12

13 **Abstract**

14 Compounding energy demand and environmental issues necessitate suitable alternative or
15 partial replacement of fossil fuels. Among the possible sources, biodiesel from non-edible
16 vegetable oil source is more economically feasible and possesses characteristics close to
17 petroleum diesel. Two potential non-edible biodiesel feedstocks “*Croton megalocarpus*” and
18 “*Ceiba pentandra*” were used for biodiesel production through esterification and
19 transesterification process in laboratory scale. Biodiesel characterization, engine performance
20 and emission characteristics were investigated in an unmodified direct injection, naturally
21 aspirated, single-cylinder diesel engine. 20% (v/v) of each *C. megalocarpus* (CM), *C.*
22 *pentandra* (CP) and their combined blends (CMB20, CPB20, CMB15CPB05,
23 CMB10CPB10, and CMB05CPB15) were tested under varying engine speed ranging from
24 1000 rpm to 2400 rpm at full load condition. CMB20 and CPB20 reduced the brake power
25 (BP) by 2.63% and 3.70%, brake thermal efficiency (BTE) by 5.97% and 3.72%, carbon

* Corresponding author. Department of Mechanical Engineering, University of Malaya, 50603, Kuala Lumpur, Malaysia.
Tel.: +603 79674448; Fax: +603 79675317 E-mail: ruhulamin07ruet@gmail.com

† Corresponding author. Department of Mechanical Engineering, University of Malaya, 50603, Kuala Lumpur, Malaysia.
Tel.: +603 79674448; Fax: +603 79675317 E-mail: masjuki@um.edu.my

26 monoxide (CO) emission by 1.09% and 2.39%, hydrocarbon (HC) emission by 1.48% and
 27 4.62% and smoke emission by 12.35% and 17.13%, respectively compared to petroleum
 28 diesel. On the other hand, CMB20 and CPB20 increased the brake specific fuel consumption
 29 (BSFC) by 9.74% and 7.63%, NO_x emission by 13.19% and 15.45%, respectively. A mixture
 30 of 10% of both biodiesels with diesels (CMB10CPB10) provides better performance and
 31 emission characteristics. CMB10CPB10 reduced BP, BTE, CO, HC and smoke by 0.53%,
 32 0.50%, 5.21%, 8.38% and 20.71%, respectively and increased BSFC and NO_x by 3.90% and
 33 18.66%, respectively than conventional diesel. Combined blend of the CM and CP could be
 34 the sustainable and substitute of fossil diesel in the context of performance and emission.

35 **Keywords:** Performance, Emission, Croton oil, Ceiba oil, Esterification, Transesterification.

36 **Nomenclature and Abbreviations**

37	BP	Brake Power
38	BSFC	Brake Specific Fuel Consumption
39	BTE	Brake Thermal Efficiency
40	CCMO	Crude <i>Croton megalocarpus</i> Oil
41	CCPO	Crude <i>Ceiba pentandra</i> Oil
42	CMB	Pure <i>Croton megalocarpus</i> biodiesel
43	CPB	Pure <i>Ceiba pentandra</i> biodiesel
44	CMB20	20% <i>Croton megalocarpus</i> biodiesel + 80% diesel
45	CPB20	20% <i>Ceiba pentandra</i> biodiesel + 80% diesel
46	CMB15CPB05	15% CMB + 05% CPB + 80% diesel
47	CMB10CPB10	10% CMB+ 10% CPB+ 80% diesel
48	CMB05CPB15	05% CMB+ 15% CPB+ 80% diesel
49	CO	Carbon monoxide
50	CO ₂	Carbon dioxide
51	CP	Cloud Point
52	CFPP	Cold Filter Plugging Point
53	CN	Cetane Number
54	FP	Flash Point
55	FFA	Free Fatty Acid
56	FAC	Fatty Acid Composition
57	FTIR	Fourier Transform Infrared Spectroscopy
58	FAME	Fatty Acid Methyl Ester
59	GC	Gas Chromatography
60	HC	Hydrocarbon
61	IV	Iodine Value
62	NO _x	Oxides of Nitrogen
63	NO	Nitric oxide

64	NO ₂	Nitrogen dioxide
65	PP	Pour Point
66	SN	Saponification Number
67		

68 **1. Introduction**

69 The consumption of fossil fuel is increasing day by day due to the increase in energy demand
70 worldwide, which results in diminishing fossil fuel reserve. The quick consumption and
71 rising costs of petroleum fuel other than their harmful emission are the primary concerns to
72 look for alternative renewable sources. Thus, research on alternative and renewable energy
73 source is always a burning issue for future energy demand fulfillment. Biofuel is one of the
74 potential alternative resources. The term biofuel refers to liquid or gaseous fuels that are
75 predominantly produced from biomass. A variety of fuels can be produced from biomass
76 resources including liquid fuels, such as bioethanol, methanol, biodiesel, Fischer–Tropsch
77 diesel, and gaseous fuels, such as hydrogen and methane¹. Biodiesel is the most convenient
78 alternative source that could play a very important role to meet the energy demand, especially
79 in automobile and power generation sector. Generally, it is synthesized from edible oils due
80 to abundance and low free fatty acid content. Biodiesel contains alkyl ester which could be
81 derived by transesterification of triglycerides or esterification of free fatty acids with lower
82 weight alcohol. On the other hand, the consideration is essentially engaged towards biodiesel
83 from non-edible feedstocks as dependency on edible source pose threat to food supply. In
84 addition, production of biodiesel from non-edible feedstocks decreases the expense of
85 biodiesel as these are fundamentally less expensive^{2, 3}. *Croton megalocarpus* and *Ceiba*
86 *pentandra* are two of the potential non-edible feedstocks which have recently drawn attention
87 of the researchers⁴⁻⁷.

88 Silitonga et al.⁴ produced biodiesel from *Ceiba pentandra* feedstock through combined acid
89 esterification and base transesterification process. For acid esterification, 1% (v/v) of H₂SO₄

90 acid catalyst, 60°C reaction temperature and 2 h reaction time was used. During base
91 transesterification, 1% (w/w) of NaOH catalyst, 50°C temperature and 2 h time was used was
92 used. In both cases they have used 8:1 methanol to oil molar ratio and 1200 rpm stirring
93 speed. They also characterized different properties of different blends of up to 50% with
94 diesel. Ong et al.⁸ and Silitonga et al.⁹ investigated engine performance and emission with
95 up to 50% *C. pentandra* biodiesel blending with diesel in every 10% composition interval.
96 They found that 10% blend provides better results in terms of torque, power, and fuel
97 consumption than other blend ratios. Vedharaj et al.¹⁰ obtained 4% superior thermal
98 efficiency than conventional diesel for 25% CPB-diesel blend. Bokhari et al.¹¹ introduced
99 the microwave-assisted technique to optimize the conversion of *C. pentandra* oil using
100 response surface methodology (RSM). They recorded optimized condition of 1:9.85 oil to
101 methanol molar ratio, 2.15 wt. % KOH catalyst loading, 57.09°C reaction temperature and
102 3.29 minute reaction time for 98.9% yield.

103 Kafuku et al.¹² investigated the production optimization and the effects of different
104 parameters of transesterification reaction during converting the methyl ester from *C.*
105 *megalocarpus*. They varied the catalyst from 0.5 wt.% to 1.5wt.% with 0.25 wt.% interval,
106 reaction time from 30 minutes to 90 minutes with 15 minute interval, methanol to oil ratio
107 from 10% (w/w) to 50% (w/w) with 10 wt. % interval, reaction temperature 30°C to 60°C
108 with 10°C interval, and stirring speed 20 rpm to 800 rpm with 200 rpm interval. They found
109 that 1 wt.% catalytic loading, 30 wt.% methanol loading and 60 minutes reaction time gives
110 an optimum yield of 90%. Aliyu et al.¹³ investigated the performance and emission
111 characteristics of *C. megalocarpus* based biodiesel on 4 stroke 3-cylinder unmodified diesel
112 engine. They found lower BTE and higher exhaust temperature for biodiesel blends compare
113 to diesel.

114 Earlier studies have addressed the suitability of the biodiesel and its blends derived from
115 these feedstocks in diesel engines. However, combined blend of multiple feedstocks are being
116 tested nowadays to improve the biodiesel economics while simultaneously enhancing fuel
117 performance ¹⁴. Habibullah et al. ¹⁵ studied the effect of 20% (v/v) palm, coconut, palm-
118 coconut (PB5CB15, PB10CB10 and PB15CB5) biodiesel and 30% (v/v) ¹⁶ palm, coconut and
119 palm-coconut (PB15CB15) biodiesel separately on an unmodified direct injection diesel
120 engine. Among 20% blends, palm-coconut combined blends reduced 0.54% to 1.85% NO_x
121 emission with slightly improved BP. Compared to 30% palm and coconut blends, PB15CB15
122 provided improved BTE and emissions except NO_x. Arbab et al. ¹⁷ optimized the palm-
123 coconut blending ratio by evaluating the combustion, performance and emission by palm-
124 coconut blend (up to 20%) in a turbocharged and non-turbocharged unmodified diesel engine.
125 They observed that combined palm-coconut blend provides superior performance and
126 emission over individual palm biodiesel-diesel blend.

127 This experimental study examines the potential of using a combined blend of *Ceiba*
128 *pentandra* and *Croton megalocarpus* biodiesel as a partial replacement for diesel fuel in a
129 single-cylinder diesel engine. These biodiesels were blended based on the difference of
130 cetane index between these two as the higher the cetane index, the better the combustion
131 properties. ASTM D7467 suggests the blending of biodiesel with diesel from 6% to 20%
132 (B6–B20). Biodiesel blends of up to 20% with diesel (B20) can be easily used in the existing
133 diesel engines without the need for engine modification ¹⁸. This study has particular relevance
134 to South East Asian region where the potential exists for availability of both of these
135 feedstocks and the establishment of economically viable application of biodiesels from these
136 oils.

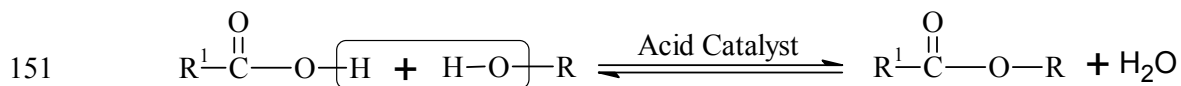
137 2. Materials and methodology

138 The crude of *C. pentandra* oil and *C. megalocarpus* oil were purchased from local markets.
 139 Highly pure analytical grade chemicals were chosen e.g. 96% pure H₂SO₄ (sulfuric acid),
 140 99.8% pure CH₃OH (methanol), 85% pure KOH (potassium hydroxide) and 99% pure
 141 Na₂SO₄ (sodium sulfate) etc. The biodiesel production was carried out through a double
 142 jacketed batch glass reactor in laboratory scale with 2100 ml capacity.

143 2.1. Esterification process

144 As the crude *C. megalocarpus* and *C. pentandra* oil both contains the high acid value (more
 145 than 4 mgKOH/g), first pretreatment or esterification process was required to lower the FFA
 146 content of vegetable oil before going through the transesterification step. Acid catalyzed
 147 esterification of vegetable oil is recommended before transesterification if the acid value
 148 equal or more than 4 mgKOH/g^{19, 20}. The basic esterification reaction of a triglycerides is
 149 representing in the **Figure 1** where R represents small alkyl group and R¹ fatty acid chains.

150



152

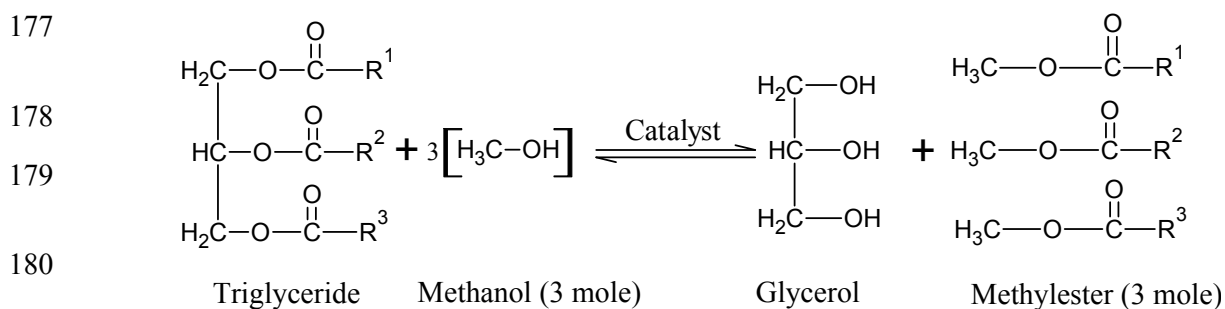
Figure 1: Basic esterification reaction

153 In this process 1000 ml crude oil from both type was taken and preheat the oil at two different
 154 batch glass reactor at 60°C to conduct the experiment. Methanol (CH₃OH) to oil molar ratio
 155 12:1 (50% v/v oil) was maintained for *C. megalocarpus* and 18:1 (75% v/v oil) for *C.*
 156 *pentandra*. After preheating and adding methanol, 1% (v/v oil) of sulfuric acid (H₂SO₄) was
 157 added and maintain 60°C reaction temperature for 3 h with 900 rpm stirring speed. After
 158 finishing the reaction, the reactants and products were poured into a separation funnel for 4h
 159 to separate excess CH₃OH, H₂SO₄ and other impurities that were presented in upper layer of
 160 the separation funnel. Esterified lower layer products were collected and removed the

161 dissolved methanol and water with the help of rotary evaporator (IKA, RV-10). 60°C water
 162 bath temperature and 339 mbar vacuum pressure for methanol removal and then 70°C
 163 temperature and 72 mbar vacuum pressure for water removal from the esterified product.
 164 This process was continued till confirming the absence of dissolved methanol and water into
 165 the esterified vegetable oil. By lowering the acid value less than 4 mgKOH/g through this
 166 process the esterified product becomes ready for transesterification.

167 2.2. Transesterification process

168 In this process the esterified *C. megalocarpus* and *C. pentandra* preheated at 60°C in
 169 different batch glass reaction and 6:1 (25% v/v oil) methanol to oil molar ratio added. 1%
 170 (w/w oil) of potassium hydroxide (KOH) was mixed as catalyst with methanol before adding
 171 with the esterified oil. Then 60°C reaction temperature was maintained for 2h under 900
 172 stirring speed. After finishing the reaction, the reactants and products were poured into a
 173 separation funnel for 12h to separate glycerol from biodiesels. This time upper layer holds
 174 desire products or biodiesel (methyl ester) and lower layer contains impurities and glycerol.
 175 An ordinary outline of the transesterification reaction for fatty acid methyl ester (FAME) is
 176 showed in **Figure 2**. Where R¹, R², R³ represents fatty acid chains ²¹.



181 **Figure 2: Basic transesterification reaction**

182 2.3. Post treatment

183 After draining the lower layer out from separation funnel, upper layer or biodiesel layer were
184 washed with 60°C warm distilled water. The washing process was including sprays warm
185 water in upper surface of the biodiesel, surface on separation funnel, shaking and stirred
186 gently. The washing process was performed several times to properly remove the impurities
187 from the produced methyl ester. Then the produced biodiesel was undergoing to the
188 mechanical and chemical drying process. For mechanical drying, a rotary evaporator was
189 used to evaporate methanol and water content from the biodiesel same condition like
190 esterification process was applied for this removal process. For chemical drying, sodium
191 sulfate anhydrous (Na_2SO_4) powder was used. Finally, the qualitative filter paper was used
192 for separating the anhydrous from the biodiesel. The filtered and clean methyl ester is the
193 desired biodiesel. It was observed that 96.5% yield and 97% yield was observed for *C.*
194 *megalocarpus* and *C. pentandra* respectively.

195 Conventional biodiesel production technology associated with higher cost compared to per
196 unit petroleum diesel production. About 60-75% biodiesel production cost is dependent on
197 the sources²². Thus non-edible and second generation biodiesel sources have more popularity
198 in the context of production cost and food security. Compared to Palm-Jatropha biodiesel
199 production from low quality feedstocks (high free fatty acid and water content present) like
200 *Ceiba* associated with higher processing cost at pretreatment and purification stage. By
201 optimizing the production process and reaction condition, the production costing could be
202 minimized about 1%-5% compared to other well-known biodiesel production like Palm or
203 *Jatropha*. *Ceiba* takes production cost around \$0.36/L whereas *Jatropha* takes \$0.36/L and
204 *Calophyllum* \$0.35/L for a 5kton capacity plant⁶.

205 **3. Physicochemical property analysis**

206 The physicochemical property of crude *C. megalocarpus* and *C. pentandra* oil were presented
 207 in Table 1. It was found that the acid value for both feedstocks are higher than 4 mgKOH/g.
 208 *C. pentandra* have the higher acid value (17.3 mg KOH/g) than *C. megalocarpus* but lower
 209 density (912.3 kg/m³) and viscosity (33.5 mm²/s) at 40°C. Also the fatty acid composition of
 210 the crude *C. megalocarpus* and the *C. pentandra* oil is represented on the **Table 1**.

211

212

213

214 **Table 1: Physicochemical property of crude *Croton megalocarpus* and *Ceiba pentandra***
 215 **oil**

216

Property	Unit	*CCMO	^a CCMO	*CCPO	^b CCPO
Density	Kg/m ³	938.5	916.8	912.3	905.2
Kinematic viscosity @40°C	mm ² /s	44.5	49.4	33.5	34.45
Acid value	mg KOH/g	4.9	4.8	17.3	16.8
FFA	%	2.46	2.45	8.69	8.44
Flash point	°C	-	-	-	170.5

^a Ref. ^{7,12}

^b Ref. ⁴

* Measured value

217

218 Fatty acid composition of the biodiesel sample was measured with the help of a GC (gas
 219 chromatographer). Agilent 7890 series, USA GC machine was used to measure the weight
 220 percentage of each FAME. **Table 2** shows the GC operation condition for measuring the
 221 FAME composition.

222

223

Table 2: GC operating condition

Parameter	Setting value/condition
Column	0.32 mm × 30 m, 0.25 μm
Injection volume	1 μL
Carrier gas	Helium, 83 kPa

Injector	Split/splitless 1177, full EFC control
Temperature	250 °C
Linear velocity	24.4 cm/s
Split flow	100 mL min ⁻¹
Column 2 flow	Helium at 1 mL min ⁻¹ constant flow
Oven	210 °C isothermal
Column temperature	60 °C for 2 min
	10 °C min ⁻¹ to 200 °C
	5 °C min ⁻¹ to 240 °C
	Hold 240 °C for 7 min
	250 °C, FID, full EFC control

224

225 It was observed that CPB contains the 28.1% saturated, 23.4% mono-unsaturated, and 48.6 %
 226 poly-unsaturated methyl ester. Among them methayl oleate (C18:1) contains 22.6% and
 227 methyl lioleate (C18:2) contains 40.7%. On the other hand, CMB contains 11.7% saturated,
 228 13.2% mono-unsaturated and 75.1% poly-unsaturated methyl ester. Among them majority
 229 portion (about 71.2%) was possessed by methyl linoleate (C18:2). It was observed that about
 230 16.3% higher unsaturated FAME contains in CMB than CPB. The details FAEM contents are
 231 presented in **Table 3**.

232 **Table 3: Fatty acid composition of *Croton megalocarpus* and *Ceiba pentandra* biodiesel**

233

FAME	Structure	Molecular weight	Composition CMB (wt. %)	Composition CPB (wt. %)
Methyl octanoate	C8:0	158.238	-	<0.1
Methyl decanoate	C10:0	186.291	-	<0.1
Methyl laurate	C12:0	214.344	-	<0.1
Methyl myristate	C14:0	242.398	<0.1	0.2
Methyl palmitate	C16:0	270.450	7.4	21.8
Methyl palmitoleate	C16:1	268.435	<0.1	0.5
Methyl heptadecanoate	C17:0	284.477	<0.1	0.1
Methyl stearate	C18:0	298.504	4.1	3.2
Methyl Oleate	C18:1	296.488	12.2	22.6
Methyl Linoleate	C18:2	294.472	71.2	40.7
Methyl linoelaidate	C18:2 isomar	294.472	-	4.1
Methyl Linolenate	C18:3	292.456	3.4	3.8
Methyl γ -Linolenate	C18:3	292.456	0.4	-
Methyl archidate	C20:0	326.557	-	0.7
Methyl icosanoate	C20:0 isomar	326.557	-	1.1
Methyl eiosenoate	C20:1	324.541	0.9	0.2

Methyl eicosadienoate	C20:2	322.525	<0.1	-
Methyl Behenate	C22:0	354.610	-	0.6
Methyl erucate	C22:1	352.594	-	<0.1
Methyl Lignocerate	C24:0	382.663	-	<0.1
Saturation			11.7 %	28.1 %
Mono-unsaturated			13.2 %	23.4 %
Poly-unsaturated			75.1 %	48.6 %
Unsaturated			88.3 %	72 %

234

235 Cetane Number (CN) were calculated from the percentage of fatty acid content, Iodine Value

236 (IV), Saponification Number (SN) and using the equation 1-3²³.

237

SN

$$= \sum \left(\frac{560 \times A_i}{MW_i} \right) \quad (1)$$

IV

$$= \sum \left(\frac{254 \times D \times A_i}{MW_i} \right) \quad (2)$$

$$\text{CN} = \left(46.3 + \left(\frac{5458}{SN} \right) - (0.225 \times IV) \right) \quad (3)$$

238 The physicochemical property of the produced biodiesel and different diesel-biodiesel blends

239 (CMB20, CMB15CPB05, CMB10CPB10, CMB05CPB15, CPB20) were determined

240 experimentally. The equipment's which were used for measuring the physicochemical

241 property characterization are represented in the **Table 4**.242 **Table 4: List of equipment used for measuring the physicochemical properties**

243

Property	Equipment description	Manufacturer	Standard	Accuracy
Density	SVM 3000-automatic	Anton Paar, UK	ASTM D127	$\pm 0.1 \text{ kg/m}^3$
Kinematic viscosity	SVM 3000-automatic	Anton Paar, UK	ASTM D445	$\pm 0.35\%$
Viscosity index	SVM 3000-	Anton Paar, UK	N/S	

Flash point	automatic Pensky-martens flash point - automatic NPM 440	Normalab, France	ASTM D93	± 0.1°C
Cloud and pour point	Automatic NTL Normalab NTE 450	Normalab, France	ASTM D2500	±0.1 °C
Cold filter plugging point	CFPP – automatic NTL 450	Normalab, France	ASTM D 6371	N/S
Acid value	G-20 Rondolino automated titration system	Mettler Toledo, Switzerland	D 664	±0.001 mgKOH/g
Calorific value	C2000 basic calorimeter – automatic	(IKA, UK)	ASTM D240	± 0.1% MJ/kg
Oxidation stability, 110 °C	Metrohm 873 Rancimat	Metrohm, Switzerland		± 0.01 hour

N/S: Not Specified

244

245 The comparison of measured result with diesel and biodiesel ASTM standard were
 246 represented in **Table 5**. All the properties were measured for three times and the average
 247 value was considered for getting more accurate result. Croton and Ceiba are of the
 248 Euphorbiaceae and Malvaceae family respectively due to which there are some
 249 physicochemical non-linearities between these two biodiesels. These non-linearities occurs
 250 mainly due to the type of their oil extraction sources (i.e. seeds). The seeds of these two shrub
 251 and tree are different in nature. Thus, they contain different type and percentage of saturated
 252 and unsaturated FAC in its crude oil. Thus, when these biodiesels are blended with diesel in
 253 different proportions, the physicochemical properties of the final blends changes according to
 254 the saturation level to each biodiesel. The degree of saturation of FAC of the final blends
 255 changes with the blending ratio. Thus, the cetane index of any blend increases when
 256 saturation percentage increases, whereas heating value increases when saturation percentage
 257 decreases of the final blends. Other properties also change in this manner.

258

259

260

261

262

263

264
265
266
267
268
269
270
271
272
273
274
275

276

277

278

279

Table 5: Physicochemical properties of *C. megalocarpus* and *C. pentandra* biodiesel and their blends

Property	Unit	ASTM	ASTM	Diesel	*CMB and *CPB blend							
		D975	6751-08		Diesel	Biodiesel	*D100	CMB	CMB20	CMB15CPB05	CMB10CPB10	CMB05CPB15
Density @40°C	kg/m ³	850 ^b	880 ^b	831.5	869.9	838.8	838.5	838.2	838.0	837.8	865.1	
Kinematic viscosity @40°C	mm ² /s	1.3-4.1	1.9-6.0	3.9016	4.1287	3.9182	3.9297	3.9386	3.9515	3.9625	4.2927	
Dynamic viscosity @40°C	mPa.S	-	-	3.2691	3.5917	3.2864	3.2949	3.3215	3.3115	3.3198	3.7137	
Acid value	mg KOH/g	-	Max. 0.5	0.247	0.334	0.281	0.269	0.270	0.257	0.333	0.447	
Iodine value	I ₂ mg/g	-	-	-	115	109	107	89	93	103	107	
Flash point	°C	60 to 80	93	79	190	88	85	83	84	86	157	
Pour point	°C	-35	-15 to 16	-3	-5	-	-	-	-	-	2.8	
Cloud point	°C	-20	-3 to 12	-2	-3	-	-	-	-	-	3	
CFPP	°C	-25	Max. 5	-6	1	-	-	-	-	-	2	
Calorific value	kJ/kg	42000-46000	-	45802	39951	44397	44349	44302	44255	44208	39001	
Oxidation stability 110 °C	h	-	Min. 3	19.89	2.65	4.16	3.68	2.87	2.46	2.24	2.15	
Cetane Index	-	40-55 ^d	Min.47 ^d	45.31 ^c	42.40 ^a	43.55 ^c	44.02 ^c	45.90 ^c	46.26 ^c	47.89 ^c	50.36 ^a	
Carbon	wt%	84-87	77	87	76.88	-	-	-	-	-	76.45	
Hydrogen	wt%	12-16	12	13	12.08	-	-	-	-	-	12.40	
Oxygen	wt%	0-0.31	11	0	11.04	-	-	-	-	-	11.14	

^a Calculated from FAC, ^b Density @15°C, ^c Calculated from ASTM 4737 method, ^d Cetane Number, * Experimental result

280

281

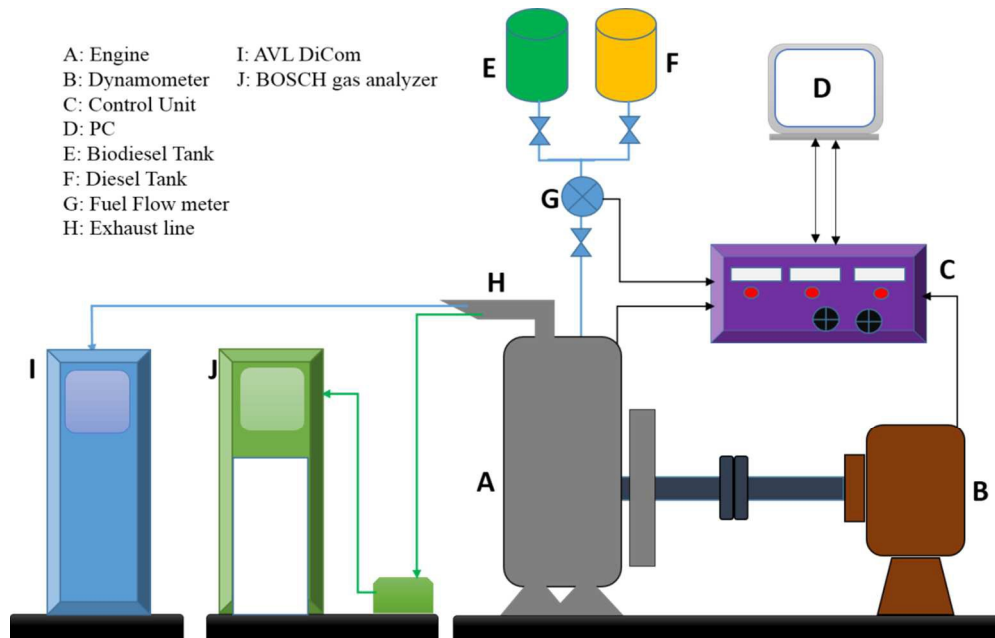
282 4. Engine test setup

283 The experiment was performed in the heat engine laboratory of the Mechanical Engineering
284 department of University of Malaya. To carry out the experiment a single-cylinder, four stroke,
285 naturally aspirated, direct injection engine was used. A pump-line-nozzle injection system was
286 integrated in the engine to inject fuel into the combustion chamber. An eddy current
287 dynamometer was coupled with the engine for setting the load condition to the engine. Besides a
288 laptop pc with Dynomax 2000 software and electronic interface was used to extract the engine
289 performance data. A digital fuel flow meter was connected with the fuel flow line to measure the
290 fuel consumption. BOSCH gas analyzer was used to measure the smoke opacity. AVL DiCom
291 4000 was connected to the engine exhaust line to measure the CO, CO₂, NO_x, and unburned HC
292 emissions. All experiment was performed in full load condition and variable speed, speed
293 variation form 1000 rpm to 2400 rpm. For a specific fuel, engine test was performed for three
294 times in each condition and the average was considered as the result value of a specific
295 condition. The engine test bed layout was presented in **Figure 3**. More details technical data of
296 the engine and dynamometer were shown on the **Table 6**.

297

298

299



300 **Figure 3: Schematic of engine test bed**

301

Table 6: Engine and Dynamometer technical specification

Engine Details			Dynamometer details	
Engine type	4 Stroke DI diesel engine		Max. Power	20kW
Number of cylinders	One		Max. Speed	10,000rpm
Aspiration	Natural aspiration		Maximum Torque	80 Nm
Cylinder bore × stroke (mm)	92×96		Water flow rate	14 L/min.
Displacement (L)	0.638		(Maximum Power)	
Compression ratio	17.7		Water pressure	23 lbf/in ²
Maximum engine speed (rpm)	2400		Electricity	220 V, 50/60 Hz, 0.5 A
Maximum power (kW)	7.7		Dynamometer control unit	
Injection timing (deg.)	17°before TDC		Accuracy	0.10%
Injection pressure (kg/cm ²)	200		Precision	0.005% ± 1 digit
Power take off position	Flywheel side		Weight measurement	Linear (load cell)
Cooling system	Radiator cooling		Speed measurement	Sensor
Connecting rod length (mm)	149.5		Operating temperature	Up to 70°C
Fuel System	Pump line nozzle injection		Operating voltage	230 VAC ± 10%, 50-60 Hz
			Output	Dynomax 2000 software with PC interface

302 **4.1. Accuracy and uncertainty analysis**

303 Instrumental accuracy and measuring uncertainty are kind of error during measuring data.

304 Accuracy is the resolution of a measuring instrument which were provided by the manufacturer

305 for a specific instrument. It indicates that how precisely the instrument can measure the value.
 306 Uncertainties in any experiments appear depending on the experimental conditions, instrument
 307 calibrations, observation, data input, test assembly etc.²⁴. Therefore, uncertainty analysis is a
 308 significant technique to validate the accuracy of the experimental results. A sample calculation
 309 for uncertainty and error analysis of brake power (BP) for diesel was presented in the Appendix
 310 “A” and “B”, respectively. In this study percentage relative uncertainty was determined by the
 311 linearized approximation method of uncertainty. However, uncertainty calculation was
 312 performed based on the three test result of each parameter as well as for each condition.

313 **Table 7** represents the other exhaust emission parameter measuring instruments with its accuracy
 314 and experimental uncertainty level. After calculating the individual uncertainty of measuring
 315 instrument, overall experimental uncertainty was computed by the equation (4).

$$\text{Overall experimental uncertainty} = \sqrt{\sum (\text{Uncertainty of each parameter})^2} \quad (4)$$

316 Overall experimental uncertainty = Square root of [(uncertainty of BP)² + (uncertainty of
 317 BSFC)² + (uncertainty of BTE)² + (uncertainty of NO_x)² + (uncertainty of CO)² + (uncertainty of
 318 HC)² + (uncertainty of Smoke)²] = Square root of [(±1.72)² + (±1.02)² + (±1.41)² + (±1.67)² +
 319 (±1.4)² + (±1.92)² + (±1.82)²] = ±4.21%

320
 321 It was observed that the overall experimental uncertainty was less than 5% (95% confidence
 322 level), which was within the acceptable range.

323

324

325
326**Table 7: Gas analyzer specification**

Equipment	Method	Measurement	Measuring range	Accuracy	% Uncertainty
AVL DiCom 4000	Electrochemical detector	NO _x	0-5000 ppm vol.	±1 ppm	±1.67%
	Non-dispersive infrared	HC	0-20000 ppm vol.	±1 ppm	±1.92%
	Non-dispersive infrared	CO	0-10% vol.	±0.01% vol.	±1.40%
	Non-dispersive infrared	CO ₂	0-20% vol.	0.1% vol.	-
	Electrochemical detector	O ₂	0-25% vol.	0.01% vol.	-
BOSCH RTM 430	Photodiode receiver	Smoke opacity	100%	±0.1%	±1.82%

327

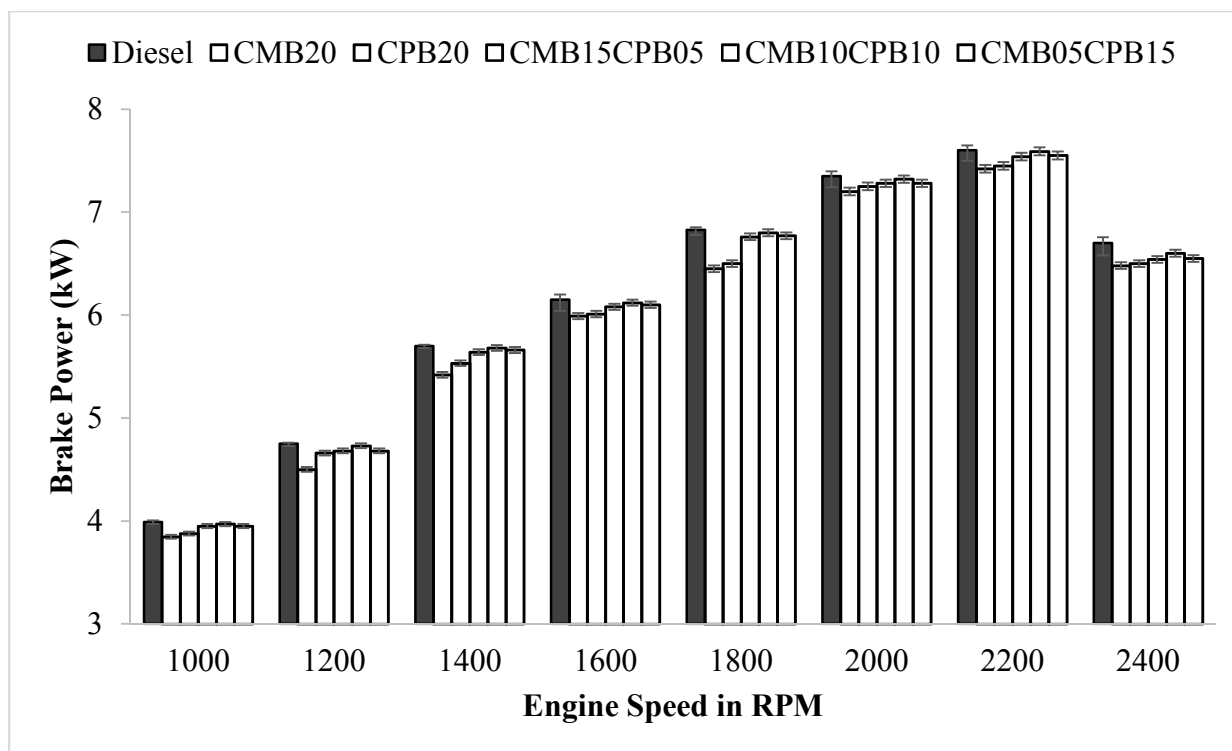
328 **5. Results and discussion**329 **5.1. Performance analysis**

330 Engine performance and fuel consumption were strongly governed by the physical and chemical
 331 properties of the fuel used. Engine performance parameters include BP, BSFC and BTE. This
 332 section represents the impact of 20% different biodiesel blends (CMB20, CMB15CPB05,
 333 CMB10CPB10, CMB05CPB15, and CPB20) of CMB and CPB in direct injection diesel engine
 334 at full throttle (100% load) condition with different engine speeds. The engine speed was varied
 335 for 1000 rpm to maximum 2400 rpm with an interval of 200 rpm.

336 **5.1.1. BP**

337 The engine performance mostly depends on fuel properties such as oxygen content, density,
 338 viscosity, calorific value etc. and fuel injection system¹⁵. Basically, these fuel property affects
 339 spray formation during fuel injection as well as it affects the combustion²⁵. **Figure 4**
 340 demonstrates the effect on BP with the variation of speed at full load condition. It was clearly
 341 observed that for both diesel and biodiesel-diesel blend BP increases with the increasing of the
 342 engine speed up to rated speed 2200 rpm. At maximum speed (2400 rpm) power output

343 decreased due to poor fuel atomization during combustion ²⁶ and increase of piston cylinder
344 frictional losses associated with higher engine speed ²⁷. Maximum BP was observed at 2200 rpm.
345 The maximum BP were recorded 7.60, 7.45, 7.42, 7.54, 7.59 and 7.55 kW for diesel, CMB20,
346 CPB20 CMB15CPB05, CMB10CPB10 and CMB05CPB15, respectively. BP output level was
347 lower (about 1.09% to 3.7%) for biodiesel blends than petro diesel in all speeds. This can be
348 attributed to combined effect of higher specific density, lower calorific value, higher viscosity
349 and lower volatility (higher flash point compared to diesel) of biodiesels ²⁸. However, combined
350 effect of this properties creates high injection in premixed region, poor fuel spray formation,
351 incomplete combustion and high global fuel-air ratio equivalence ratio for lowering the BP of
352 biodiesel blends than petro diesel ^{19, 29}. This result, together with almost 12.07% lower calorific
353 value of biodiesels can be attributed to the lower BP output than diesel. Among all the 20%
354 biodiesel blends CMB10CPB10 showed the higher BP output at higher engine speed. This
355 outcome may be attributed to the combined effect of the density and viscosity that diminish the
356 inner spillage in the pump ^{30, 31} and flash point that affects atomization or spray formation of fuel
357 during combustion. Another reason could be the combined effect of additional oxygen content
358 in biodiesels ¹⁷ and improvements of CN of combined blends. Accumulating lowest calorific
359 value among all the combined blends, CPB20 demonstrated somewhat least BP. Addition of
360 CPB with CMB improves the Cetane Index as well as the BP of the engine.



361

362

Figure 4. Brake power vs. engine speed for full load condition

363 5.1.2. BSFC

364 BSFC is defined as fuel consumption per unit BP output for a specific fuel. Fuel properties e.g.

365 density, viscosity and calorific value have significant influences on engine BSFC. **Figure 5**

366 illustrates the BSFC in g/kWh with variation of engine speed. The figure shows that BSFC of

367 biodiesel blends is higher than that of petro diesel. This may be attributed to higher density and

368 viscosity of biodiesel compared to diesel ³². The figure also demonstrates that initially the BSFC

369 for all fuels gradually decreased with increasing engine speed till 1800 rpm. This may be

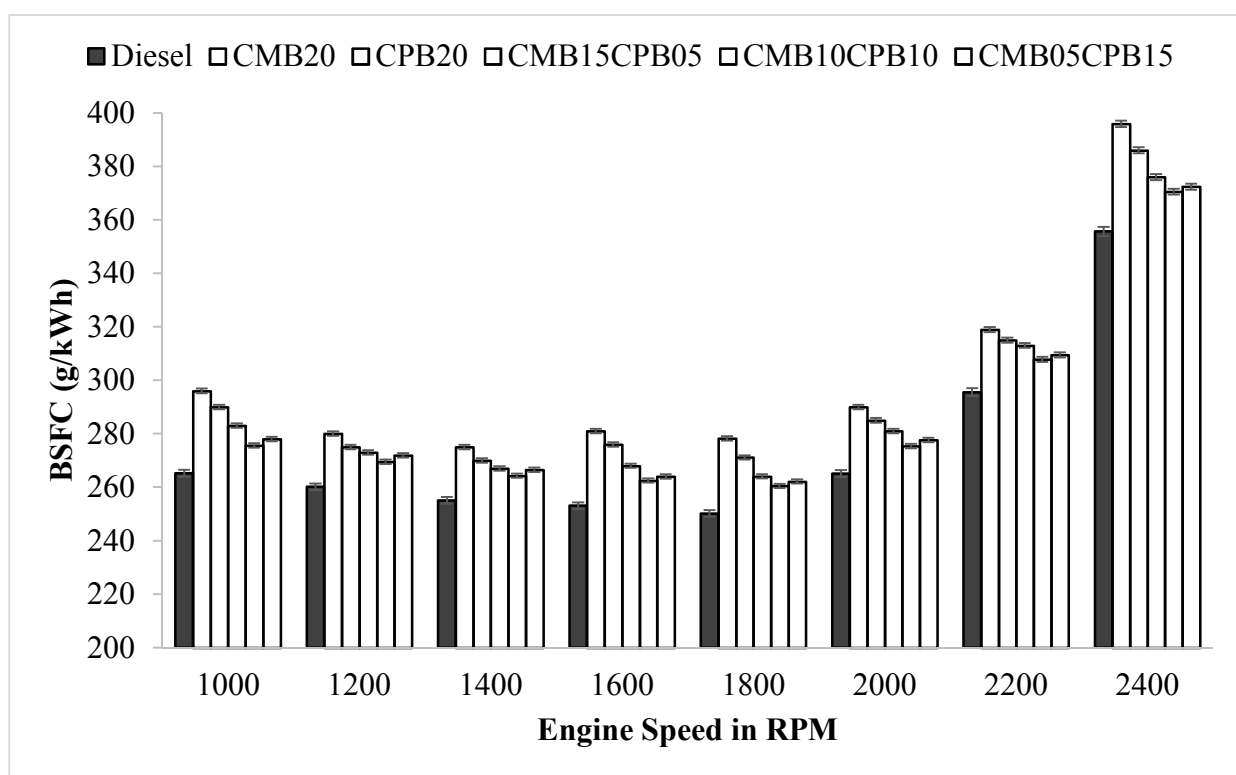
370 attributed to increased fuel atomization ratio, subsequently, the air-fuel equivalence ratio, which

371 influences air and fuel mixing ¹⁵. The lowest BSFC for diesel, CMB20, CPB20, CMB15CPB05,

372 CMB10CPB10 and CMB05CPB15 were recorded 250.16, 278.23, 271.14, 264.05, 260.50 and

373 262.10 g/kWh, respectively at 1800 rpm. BSFC gradually increased with the engine speed after

374 1800rpm. Maximum BSFC for diesel, CMB20, CPB20, CMB15CPB05, CMB10CPB10 and
 375 CMB05CPB15 were recorded 355.62, 395.93, 386.00, 376.10, 370.53 and 372.41 g/kWh,
 376 respectively at the maximum engine speed (2400 rpm). Volumetric efficiency decrease and
 377 increased frictional loss at higher speed might be the reason for this increase. In addition, BSFC
 378 increases with increasing engine speed and blend ratio of biodiesel ²⁶. Higher density and
 379 viscosity of biodiesel blends leads to higher mass flow rate in mechanically controlled pump-
 380 line-nozzle system as fuel is injected volumetrically affecting the fuel atomization³³. Individual
 381 blends of CMB and CPB possess higher density and viscosity respectively, rather than combined
 382 blends which results in higher BSFC. With increasing amount of CPB in blend results in lower
 383 density but increased viscosity, which in turn increased surface tension of the blend. This
 384 resulted in a decrease in BSFC.



385

386

Figure 5. BSFC vs. engine speed for full load condition

387 5.1.3. BTE

388 BTE is defined as break power of heat engine as a function of the heat input by the fuel. **Figure**
389 **6** shows the BTE for all tested diesel and biodiesel-diesel blends. The graphs demonstrated that
390 BTE increased with engine speed up to 1800 rpm. This outcome is usually attributed for the
391 highest BSFC was attained due to the consolidated impact of poor fuel atomization time and
392 elevated piston-cylinder frictional force at this speed ³⁴. The height BTE value for diesel,
393 CMB20, CPB20, CMB15CPB05, CMB10CPB10 and CMB05CPB15 were recorded 31.42%,
394 29.14%, 30.03%, 30.74%, 31.19% and 31.04, respectively. After 1800 rpm, BTE eventually
395 decreased along with engine speed and achieved the lowest value at 2400 rpm for each of the
396 investigated fuels. This results attributed to the higher fuel consumption for the increased engine
397 speed. Compared to diesel maximum BTE of biodiesel-diesel blend were decreased by 0.50% to
398 5.97%. This changes due to the fuel variation were significant. BTE changed with the variety in
399 BSFC and calorific value of the biodiesel. Though individual CMB20 possess higher calorific
400 value that CPB20 as well as opposite for viscosity and CN, thus CMB20 showed lower BTE than
401 CPB20. On the other hand, combined blending provides better combination of density, viscosity
402 as well as CN rather than individual biodiesel (CMB20 and CPB20) blends. Addition of higher
403 percentage of CPB with CMB increases BTE and thus 10% combined blend of CMB and CPB
404 provides the higher BTE as well as the lower BSFC among the biodiesel-biodiesel blends.
405 Combustion phasing additionally impacts the energy conversion of heat energy to work. Quick
406 injection of biodiesel together with high CN results in the early start of combustion (SOC) ³⁵.
407 Early SOC, raises pumping function and endorses heat decrease in the cycle ^{31, 33}. This trend,
408 collectively along with low heating value and higher density, viscosity, negatively impacts
409 engine performance ^{36, 37}.

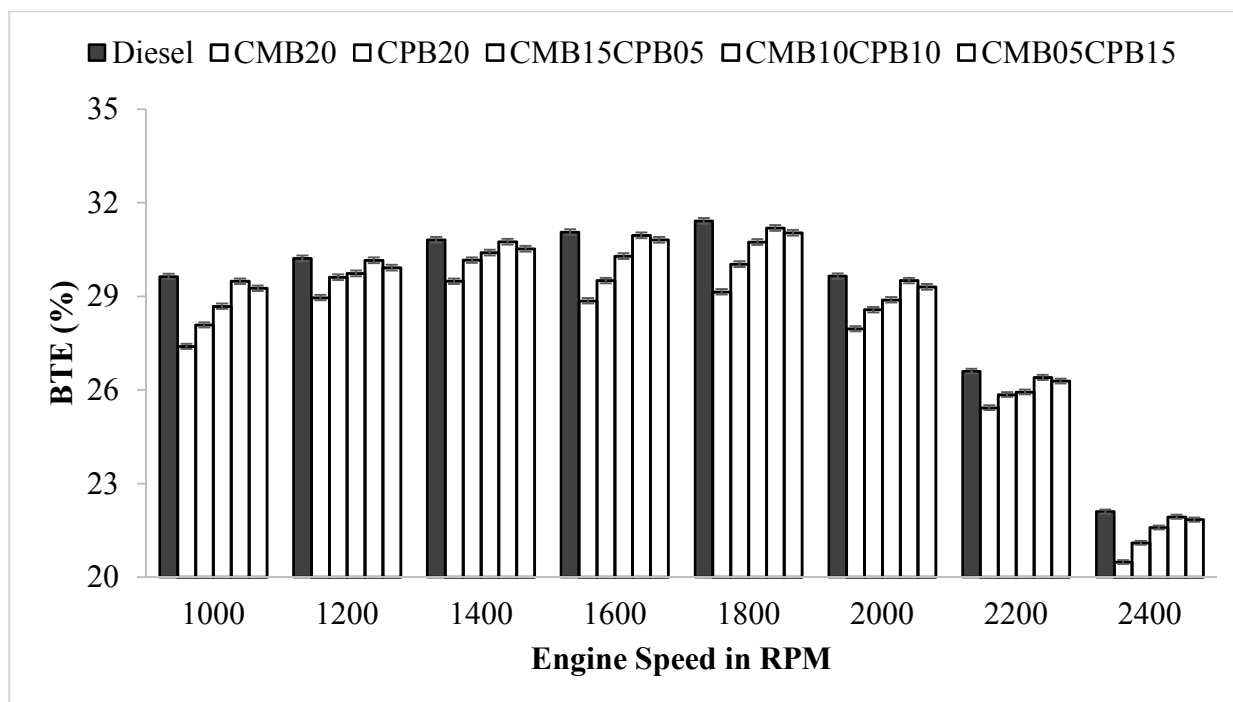


Figure 6. BTE vs. engine speed for full load condition

410

411

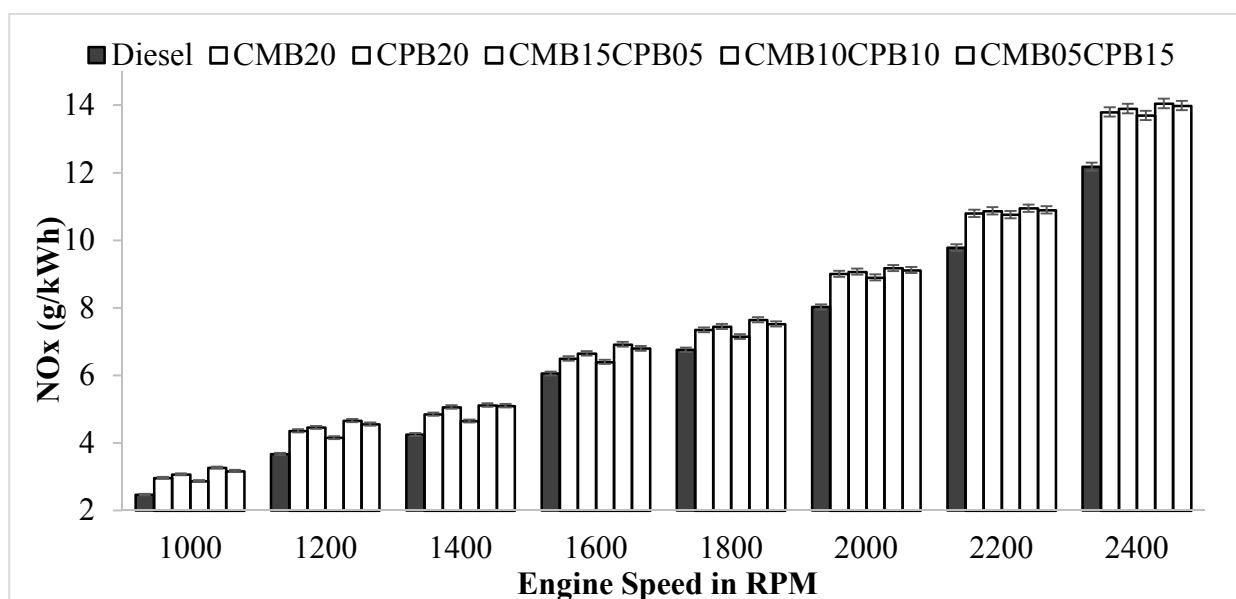
412 5.2. Emission analysis

413 Emission parameter such as NO_x , CO, HC and Smoke opacity were investigated throughout the
414 experiments.

415 5.2.1. NO_x

416 NO_x emission mainly includes nitric oxide (NO) and nitrogen dioxide (NO_2) emission to the
417 environment. NO is the prevalent oxide delivered inside the engine cylinder. During combustion,
418 atmospheric nitrogen (about 78.09% by volume) come into reaction and become the main source
419 for NO_x emission for the internal combustion engine, this is treated as the thermal NO_x .
420 Atmospheric triple bonded nitrogen behaves as an inert gas but in high combustion temperature
421 it splits up and undergoes with a series of reaction with oxygen and creates NO_2 . This NO_x
422 formation mechanism is known as Zeldovich mechanism. NO_x forms in prompt (Fenimore)
423 mechanism because of the generation of hydrocarbon radicals via molecular unsaturation^{38, 39}.

424 **Figure 7** demonstrate the NO_x emission for variable speed for full load. NO_x was gradually
 425 increasing with engine speed as the combustion temperature increase, with higher engine speed.
 426 The highest NO_x emission were observed for diesel, CMB20, CPB20, CMB15CPB05,
 427 CMB10CPB10 and CMB05CPB15 were recorded 12.18, 13.80, 13.90, 13.70, 14.05 and 13.99
 428 g/kWh, respectively at 2400 rpm. NO_x formation through the biodiesel blend is quite high due to
 429 12-13 % higher oxygen content in biodiesel, which provides high in-cylinder temperature for
 430 both premixed and diffusion combustion condition rather than diesel⁴⁰. Together with higher
 431 CN, air surplus co-efficient, residence time and higher bulk modulus of elasticity can be ascribed
 432 as the reason for NO_x formation^{41,42}. Bulk modulus of elasticity causes the early nozzle opening
 433 and advancement of the ignition, which increase global fuel-air equivalence⁴³. Higher CN
 434 provides shorter ignition delay and higher oxygen content in biodiesel results higher combustion
 435 temperature. Because of the higher in-cylinder temperature during combustion CMB10CPB10
 436 gives slightly higher and CMB15CPB05 provides relatively lower NO_x emission among the
 437 tested biodiesel blends.



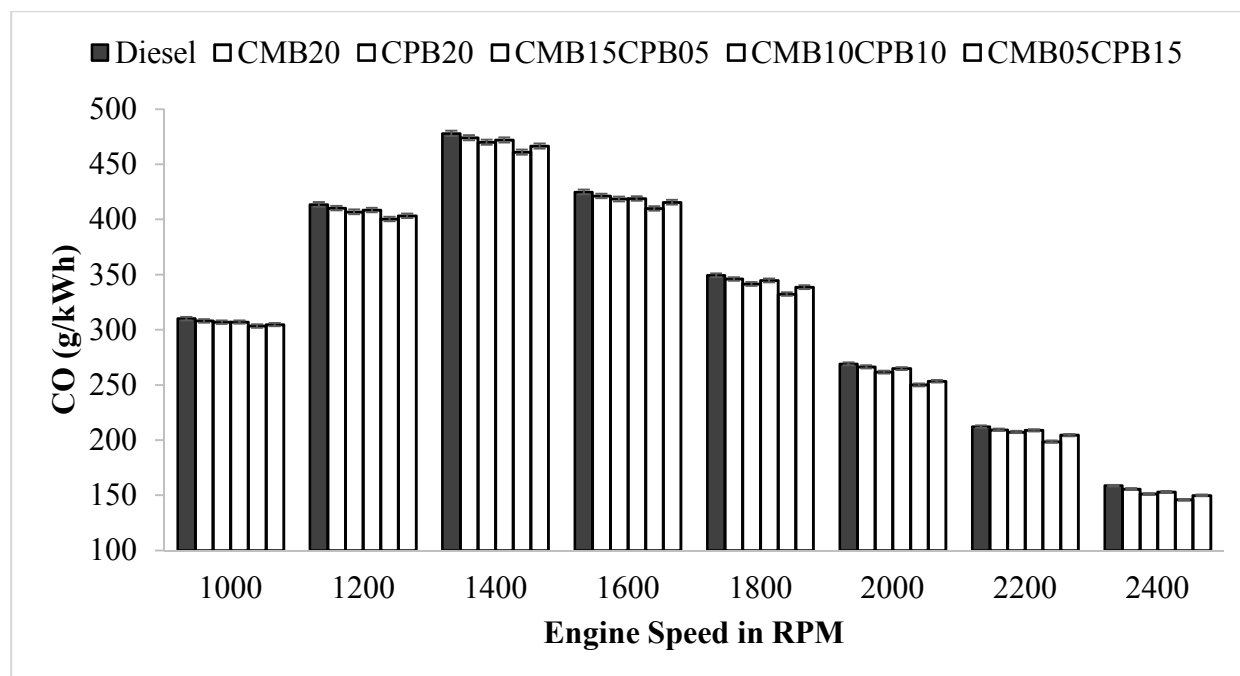
438

439

Figure 7. NO_x emission vs. engine speed for full load condition

440 5.2.2. CO

441 The partial combustion is the real cause of higher CO content in exhaust emissions ,which
442 caused by insufficient oxygen supply ⁴⁴ during combustion. All this happens because of engine
443 speed, air-fuel equivalence ratio, fuel pressure, fuel type and injection timing. Among them,
444 ignition mixture because of lower air-fuel equivalence ratio can be considered as the main cause
445 of CO emissions. **Figure 8** illustrates CO variation in different engine speeds at full load
446 condition. Initially CO emission increased with increasing the engine speed ranging from
447 1000rpm to 1400rpm. This can be attributed to the lower air-fuel equivalence ratio, lower
448 combustion temperature, poor atomization due to density, viscosity and flash point at low speed.
449 On the other hand, at higher speed (after 1800rpm) BSFC was found higher for biodiesel. With
450 increasing of engine speed, higher air-fuel equivalence ratio, higher cylinder temperature and
451 pressure was introduced during combustion, which ensures relatively better combustion and thus
452 reduced the CO emission ^{31, 45}. Overall biodiesel and biodiesel-diesel blends provides relatively
453 lower CO emission in every speeds. This can be ascribed as higher oxygen content and higher
454 CN of biodiesel, which shorting the ignition delay, thus provides better combustion and prevents
455 less over-lean zones ⁴⁶. Maximum CO emission for diesel, CMB20, CPB20, CMB15CPB05,
456 CMB10CPB10 and CMB05CPB15 were recorded 474.04, 469.97, 472.00, 461.13 and 466.51
457 g/kWh, respectively at 1400 rpm. CO emission reduction for the biodiesel were obtained 1.09%
458 to 5.21% with compare to diesel.



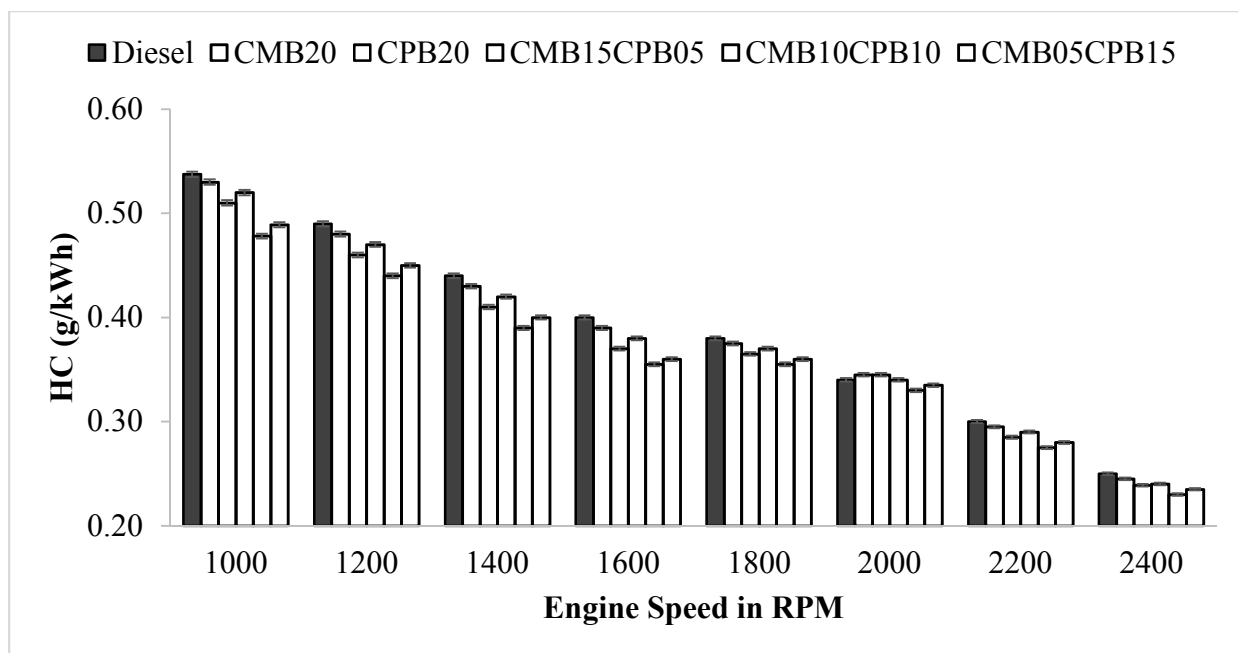
459

460

Figure 8. CO emission vs. engine speed for full load condition

461 5.2.3. HC

462 The reasonable factors that creates the HC emission for petro diesel are fuel trapping in the
 463 crevice volume of combustion³⁵, low temperature bulk quenching of oxidation reaction, locally
 464 over-lean or over-rich mixture, liquid wall filaments for excessive spray impingement and
 465 incomplete fuel evaporation⁴⁷. The **Figure 9** illustrates the HC emission; it shows alike CO
 466 emission reduction. HC emission gradually decreases with increasing engine speed. It happens
 467 because of presence of oxygenate compounds in biodiesel. Also. This can be attributed to high
 468 in-cylinder temperature due to the high in cylinder pressure⁴⁸. The maximum HC emission for
 469 diesel, CMB20, CPB20, CMB15CPB05, CMB10CPB10 and CMB05CPB15 were recorded as
 470 0.537, 0.530, 0.513, 0.524, 0.484 and 0.496 g/kWh, respectively at 1000 rpm. Compare with
 471 petro diesel, biodiesel blends and combined biodiesel blends reduces HC emission ranging from
 472 1.48% to 8.38%. The biodiesel blend CMB10CPB10 gives the lowest HC emission.



473

474

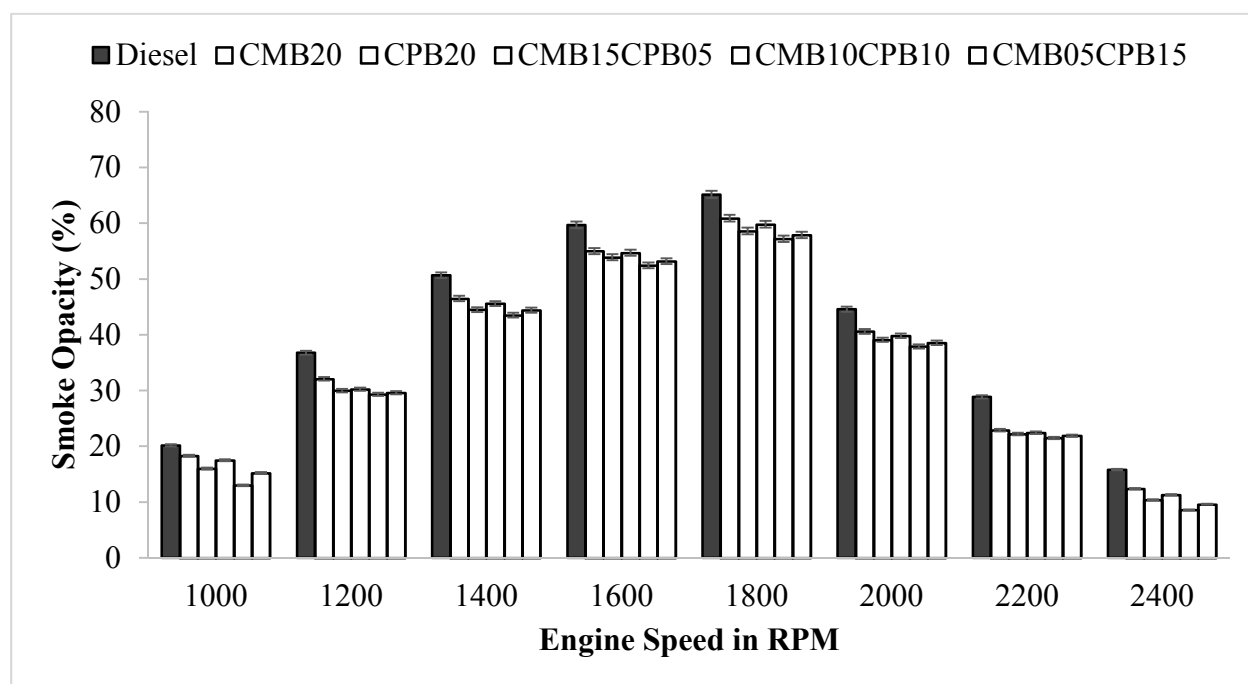
Figure 9. HC emission vs. engine speed for full load condition

475 5.2.4. Smoke opacity

476 Smoke emission refers to dark-black smoke or dry soot which is one of the principal source of
 477 particulate matter ¹⁹. Smoke emission can be measured by the term smoke opacity. **Figure 10**
 478 illustrate the smoke opacity of diesel and biodiesel-diesel blend at variable engine speed. It
 479 shows smoke opacity of all blends of biodiesel is lower than petro diesel for all the engine speed
 480 due to oxygenated biodiesel fuel structure ⁴⁹. Inborn oxygen of biodiesel provides better
 481 combustion, thus lowering the smoke emissions than diesel ⁴¹. Smoke emission gradually
 482 increases up to certain speed (in this case up to 1800rpm), then gradually decreases up to
 483 maximum speed. The increases smoke opacity can be attributed to incomplete combustion of the
 484 hydrocarbon fuel and partial reaction of the carbon content in the liquid fuel ²⁸ due to lower
 485 combustion temperature and poor atomization (due to density, viscosity and flash point) at low
 486 speed ranging from 1000 rpm to 1800rpm. Maximum smoke opacity for diesel, CMB20, CPB20,

487 CMB15CP05, CMB10CPB10, CMB05CPB15 were recorded 65.15%, 60.90%, 58.60%, 59.80%,
 488 57.20% and 57.90%, respectively at 1800 rpm. After 1800rpm, air-fuel equivalence ratio
 489 increases with engine speed and introduced higher combustion temperature which provides
 490 better burning of HC during combustion, thus decreased smoke opacity. However, Tested
 491 biodiesel blends provides on an average 12.35% to 20.71% smoke emission reduction than petro
 492 diesel. Addition of CPB in CMB leads to an increase in viscosity and decrease in density, thus
 493 provides better BSFC and fuel atomization. Among all tested biodiesels and combined biodiesel
 494 blends, CMB10CPB10 provides slightly lower smoke opacity.

495



496

497 **Figure 10. Smoke opacity vs engine speed for full load condition**

498 6. Conclusions

499 In this study biodiesel was produced from *C. megalocarpus* and *C. pentandra* feedstock and their
 500 physiochemical properties were examined. In addition, performance and emission characteristics

501 of 20% biodiesel-diesel blend of CMB & CPB together with their combined blend were
502 considered. These biodiesels were blended based on the difference of cetane index between these
503 two as the higher the cetane index, the better the combustion properties. From the above
504 experimental observation following conclusion can be drawn: -

505 Compared to ordinary diesel, for all tested blends

- 506 • The average engine brake power was lower about 0.53% to 3.70%.
- 507 • BSFC were higher about 3.90% to 9.74% than that of diesel mainly owing to their lower
508 heating value and higher density and viscosity.
- 509 • The BTE were slightly lower (about 0.50%-5.97%).
- 510 • The average NO_x emission were 10.50% to 18.66% higher.
- 511 • The CO and HC emissions were reduced to an extent of 1.09%-5.21% and 1.48%-8.38%.

512 In conclusion, the lower brake power output from burning of *C. megalocarpus* biodiesel blends
513 can be improved by the addition of *C. pentandra* biodiesel. At the same time, they slightly
514 improve all emission except NO_x. Further research could be done by introducing some additives
515 for improving the NO_x emission and the stability of the biodiesel blends.

516 **Acknowledgement**

517 The authors would like to thank the University of Malaya for financial support through High Impact
518 Research grant titled: Development of Alternative and Renewable Energy Carrier (DAREC) having Grant
519 Number UM.C/HIR/MOHE/ENG/60 and University Malaya Research Grant (UMRG) having Grant
520 number RP016-2012B.

521 **References**

- 522 1. S. A. Shahir, H. H. Masjuki, M. A. Kalam, A. Imran, I. M. R. Fattah and A. Sanjid,
523 *Renewable and Sustainable Energy Reviews*, 2014, **32**, 379-395.
- 524 2. A. E. Atabani, T. M. I. Mahlia, H. H. Masjuki, I. A. Badruddin, H. W. Yussof, W. T.
525 Chong and K. T. Lee, *Energy*, 2013, **58**, 296-304.
- 526 3. M. Tabatabaei, K. Karimi, I. S. Horváth and K. Rajeev, *Biofuel Research Journal*, 2015,
527 **2**, 258-267.
- 528 4. A. S. Silitonga, H. C. Ong, T. M. I. Mahlia, H. H. Masjuki and W. T. Chong, *Fuel*, 2013,
529 **108**, 855-858.
- 530 5. T. M. Y. Khan, A. E. Atabani, I. A. Badruddin, R. F. Ankalgi, T. K. M. Khan and A.
531 Badarudin, *Industrial Crops and Products*, 2015, **65**, 367-373.
- 532 6. H. Ong, A. Silitonga, H. Masjuki, T. Mahlia, W. Chong and M. Boosroh, *Energy*
533 *conversion and management*, 2013, **73**, 245-255.
- 534 7. G. Kafuku, M. K. Lam, J. Kansedo, K. T. Lee and M. Mbarawa, *Bioresource technology*,
535 2010, **101**, 7000-7004.
- 536 8. H. C. Ong, H. H. Masjuki, T. M. I. Mahlia, A. S. Silitonga, W. T. Chong and T. Yusaf,
537 *Energy*, 2014, **69**, 427-445.
- 538 9. A. Silitonga, H. Masjuki, T. Mahlia, H. C. Ong and W. Chong, *Energy Conversion and*
539 *Management*, 2013, **76**, 828-836.
- 540 10. S. Vedharaj, R. Vallinayagam, W. M. Yang, S. K. Chou, K. J. E. Chua and P. S. Lee,
541 *Energy Conversion and Management*, 2013, **75**, 773-779.
- 542 11. A. Bokhari, L. F. Chuah, Y. Suzana, A. Junaid, M. R. Shamsuddin and M. K. Teng,
543 *Biofuel Research Journal*, 2015, **2**, 281-287.
- 544 12. G. Kafuku and M. Mbarawa, *Fuel*, 2010, **89**, 2556-2560.
- 545 13. B. Aliyu, D. Shitanda, S. Walker, B. Agnew, S. Masheiti and R. Atan, *Applied Thermal*
546 *Engineering*, 2011, **31**, 36-41.
- 547 14. B. R. Moser, *Renewable Energy*, 2016, **85**, 819-825.
- 548 15. M. Habibullah, I. Rizwanul Fattah, H. Masjuki and M. Kalam, *Energy & Fuels*, 2015, **29**,
549 734-743.
- 550 16. M. Habibullah, H. H. Masjuki, M. A. Kalam, I. M. Rizwanul Fattah, A. M. Ashraful and
551 H. M. Mobarak, *Energy Conversion and Management*, 2014, **87**, 250-257.
- 552 17. M. I. Arbab, M. Varman, H. H. Masjuki, M. A. Kalam, S. Imtenan, H. Sajjad and I. M.
553 Rizwanul Fattah, *Energy Conversion and Management*, 2015, **90**, 111-120.
- 554 18. M. Kalam, H. Masjuki, M. Jayed and A. Liaquat, *Energy*, 2011, **36**, 397-402.
- 555 19. I. M. Rizwanul Fattah, M. A. Kalam, H. H. Masjuki and M. A. Wakil, *RSC Advances*,
556 2014, **4**, 17787-17796.
- 557 20. I. M. Rizwanul Fattah, H. H. Masjuki, M. A. Kalam, M. A. Wakil, H. K. Rashedul and
558 M. J. Abedin, *Industrial Crops and Products*, 2014, **57**, 132-140.
- 559 21. G. Moradi, M. Mohadesi, M. Ghanbari, M. Moradi, S. Hosseini and Y. Davoodbeygi,
560 *Biofuel Research Journal*, 2015, **2**, 236-241.
- 561 22. A. Ruhul, M. Kalam, H. Masjuki, I. R. Fattah, S. Reham and M. Rashed, *RSC Advances*,
562 2015, **5**, 101023-101044.
- 563 23. K. Krisnangkura, *Journal of the American Oil Chemists Society*, 1986, **63**, 552-553.
- 564 24. M. A. Kalam and H. H. Masjuki, *Energy*, 2011, **36**, 3563-3571.
- 565 25. S. Murillo, J. Miguez, J. Porteiro, E. Granada and J. Moran, *Fuel*, 2007, **86**, 1765-1771.

- 566 26. I. R. Fattah, H. Masjuki, M. Kalam, M. Wakil, A. Ashraful and S. A. Shahir, *Energy*
567 *Conversion and Management*, 2014, **83**, 232-240.
- 568 27. M. A. Kalam, H. H. Masjuki, M. H. Jayed and A. M. Liaquat, *Energy*, 2011, **36**, 397-402.
- 569 28. H. How, H. Masjuki, M. Kalam, Y. Teoh and M. Abdullah, *Effect of Injection Timing on*
570 *Performance, Emission and Combustion Characteristics of a Common-Rail Diesel*
571 *Engine Fuelled with Coconut Oil Methyl Ester*, SAE Technical Paper, 2013.
- 572 29. Z. Chen, Z. Wu, J. Liu and C. Lee, *Energy Conversion and Management*, 2014, **78**, 787-
573 795.
- 574 30. E. Buyukkaya, S. Benli, S. Karaaslan and M. Guru, *Energy Conversion and*
575 *Management*, 2013, **69**, 41-48.
- 576 31. Ö. Can, *Energy Conversion and Management*, 2014, **87**, 676-686.
- 577 32. M. I. Arbab, H. H. Masjuki, M. Varman, M. A. Kalam, H. Sajjad and S. Imtenan, *RSC*
578 *Advances*, 2014, **4**, 37122-37129.
- 579 33. F. Payri, J. M. Desantes and J. Benajes, *Handbook of Clean Energy Systems*.
- 580 34. S. Imtenan, H. Masjuki, M. Varman, I. R. Fattah, H. Sajjad and M. Arbab, *Energy*
581 *Conversion and Management*, 2015, **94**, 84-94.
- 582 35. S. Imtenan, H. Masjuki, M. Varman and I. R. Fattah, *RSC Advances*, 2015, **5**, 17160-
583 17170.
- 584 36. S. H. Park, J. Cha and C. S. Lee, *Applied Energy*, 2012, **99**, 334-343.
- 585 37. P. Devan and N. Mahalakshmi, *Applied Energy*, 2009, **86**, 675-680.
- 586 38. P. Benjumea, J. R. Agudelo and A. F. Agudelo, *Energy & Fuels*, 2010, **25**, 77-85.
- 587 39. H. Sharon, K. Karuppasamy, D. S. Kumar and A. Sundaresan, *Renewable Energy*, 2012,
588 **47**, 160-166.
- 589 40. D. Kannan, S. Pachamuthu, M. N. Nabi, J. E. Hustad and T. Løvås, *Energy Conversion*
590 *and Management*, 2012, **53**, 322-331.
- 591 41. S. Imtenan, H. H. Masjuki, M. Varman, M. A. Kalam, M. I. Arbab, H. Sajjad and S. M.
592 Ashrafur Rahman, *Energy Conversion and Management*, 2014, **83**, 149-158.
- 593 42. I. M. Rizwanul Fattah, M. H. Hassan, M. A. Kalam, A. E. Atabani and M. J. Abedin,
594 *Journal of Cleaner Production*, 2014, **79**, 82-90.
- 595 43. A. L. Boehman, D. Morris, J. Szybist and E. Esen, *Energy & Fuels*, 2004, **18**, 1877-1882.
- 596 44. S. S. Reham, M. A. Kalam, I. Shancita, H. H. Masjuki, I. M. Rizwanul Fattah and A. M.
597 Ruhul, *Renewable and Sustainable Energy Reviews*, 2015, DOI:
598 10.1016/j.rser.2015.08.013.
- 599 45. C. Sayin, *Fuel*, 2010, **89**, 3410-3415.
- 600 46. A. Sanjid, H. H. Masjuki, M. A. Kalam, S. M. A. Rahman, M. J. Abedin, M. I. Reza and
601 H. Sajjad, *Procedia Engineering*, 2014, **90**, 397-402.
- 602 47. J. B. Heywood, *Internal combustion engine fundamentals*, Mcgraw-hill New York, 1988.
- 603 48. I. Shancita, H. Masjuki, M. Kalam, S. Reham, A. Ruhul and I. Monirul, *RSC Advances*,
604 2016, **6**, 8198-8210.
- 605 49. H. J. Curran, E. M. Fisher, P.-A. Glaude, N. M. Marinov, W. Pitz, C. Westbrook, D.
606 Layton, P. F. Flynn, R. P. Durrett and A. Zur Loye, *Detailed chemical kinetic modeling*
607 *of diesel combustion with oxygenated fuels*, Report 0148-7191, SAE Technical Paper,
608 2001.
- 609

610

Appendix

611

612 **Appendix A: Uncertainty level calculation of BP, BSFC and BTE for diesel**

Power	Three test			Max. and Min. value		Accuracy (± 0.07 kW)		Average	% Uncertainty	
	Test 1 kW	Test 2 kW	Test 3 kW	Max. kW	Min. kW	Max.+0.07	Min.-0.07		+	-
RPM	A	B	C	D	E	F=D+0.03	G=E-0.03	H=(F+G)/2	I=((F-H)/H) *100	J=((H-G)/H) *100
1000	3.98	3.98	4.00	4.00	3.98	4.07	3.91	3.99	2.01	-2.01
1200	4.74	4.75	4.76	4.76	4.74	4.83	4.67	4.75	1.68	-1.68
1400	5.69	5.70	5.71	5.71	5.69	5.78	5.62	5.70	1.40	-1.40
1600	6.09	6.16	6.20	6.20	6.09	6.27	6.02	6.14	2.03	-2.03
1800	6.83	6.80	6.85	6.85	6.8	6.92	6.73	6.82	1.39	-1.39
2000	7.29	7.40	7.37	7.40	7.29	7.47	7.22	7.34	1.70	-1.70
2200	7.55	7.61	7.65	7.65	7.55	7.72	7.48	7.60	1.58	-1.58
2400	6.64	6.71	6.76	6.76	6.64	6.83	6.57	6.70	1.94	-1.94
Uncertainty level of BP for diesel =									+1.72%	-1.72%
Similarly, uncertainty level of BSFC for diesel =									+1.02%	-1.02%
Uncertainty level of BTE for diesel=									+1.41%	-1.41%

613

614

615 **Appendix B: Sample calculation of the error bar for Power of diesel**

	Test 1 kW	Test 2 kW	Test 3 kW	Average	Maximum value	Minimum value	+ve Error	-ve Error
RPM	A	B	C	D=(A+B+C)/3	E	F	G=E-D	H=D-F
1000	3.98	3.98	4	3.99	4.00	3.98	0.01	0.02
1200	4.74	4.75	4.76	4.75	4.76	4.74	0.01	0.02
1400	5.69	5.7	5.71	5.70	5.71	5.69	0.01	0.02
1600	6.09	6.16	6.2	6.15	6.20	6.09	0.05	0.11
1800	6.83	6.8	6.85	6.83	6.85	6.80	0.02	0.05
2000	7.29	7.4	7.37	7.35	7.40	7.29	0.05	0.11
2200	7.55	7.61	7.65	7.60	7.65	7.55	0.05	0.10
2400	6.64	6.71	6.76	6.70	6.76	6.64	0.06	0.12
Average error =							0.03	0.07

616

617

618 Appendix C: Sample of Calculated Cetane Index for diesel (ASTM D4737-10)

Distillation Test result (ASTM D86)			Density, D @ 15°C (D4052)	DN (D-0.85)	B ([e ^{(-3.5)(DN)}] - 1)	T _{10N} (T ₁₀ - 215)	T _{50N} (T ₅₀ - 260)	T _{90N} (T ₉₀ - 310)
Test Parameter	Unit	Result	g/mL	g/mL		°C	°C	°C
Initial Boiling Point	°C	177.5						
5%	°C	216.8						
10%	°C	232.7						
20%	°C	252.7						
30%	°C	266.7						
40%	°C	278.0						
50%	°C	289.2						
60%	°C	301.4	0.8526	0.0026	-0.00906	17.7	29.2	39.3
70%	°C	314.6						
80%	°C	329.7						
90%	°C	349.3						
95%	°C	367.1						
Final Boiling Point	°C	374.0						
Residue	%	1.5						
Recovery	%	98						
Loss	%	0.5						

$$CCI = 45.2 + (0.0892) (T_{10N}) + [0.131 + (0.901) (B)] [T_{50N}] + [0.0523 - (0.420) (B)] [T_{90N}] + [0.00049] [(T_{10N})^2 - (T_{90N})^2] + (107) (B) + (60) (B)^2$$

Where, CCI= Calculated Cetane Index by Four Variable Equation, D = Density at 15°C, g/mL, $DN = D - 0.85$, $B = [e^{(-3.5)(DN)}] - 1$, T_{10} = 10 % recovery temperature, °C, $T_{10N} = T_{10} - 215$, T_{50} = 50 % recovery temperature, °C, $T_{50N} = T_{50} - 260$, T_{90} = 90 % recovery temperature, °C, $T_{90N} = T_{90} - 310$.

Calculate Cetane Index for Pure Diesel = **45.31**

619

620

621

622